Journal of Fluids and Structures (2000) **14,** 339–357
doi:10.1006/jfls.1999.0272, available online at http://www.idealibrary.com on IDEAL®

COUPLED VIBRATORY CHARACTERISTICS OF A RECTANGULAR CONTAINER BOTTOM PLATE

Y. K. CHEUNG

Department of Civil Engineering, The University of Hong Kong, Hong Kong

AND

D. ZHOU

School of Mechanical Engineering, Nanjing University of Science and Technology Nanjing 210014, People's Republic of China

(Received 1 February 1999, and in final form 22 October 1999)

The natural frequencies of an elastic thin plate placed into a rectangular hole and connected to the rigid bottom slab of a rectangular container filled with fluid having a free surface are studied. The fluid is assumed to be incompressible, inviscid and irrotational, and the effect of surface waves is neglected. An analytical-Ritz method is developed to study the vibratory characteristics of the plate in contact with the fluid. First of all, the exact expression of the motion of the fluid is obtained, in which the unknown coefficients are determined by using the method of separation of variables and the method of Fourier series expansion. Then, the Ritz approach is used to obtain the frequency equation of the system. The vibrating beam functions are adopted as the admissible functions for the wet-mode expansion of the plate, and the added virtual mass incremental (AVMI) matrices are obtained for plates with arbitrary boundary conditions. Finally, a convergence study is carried out and some numerical results are given. The accuracy of AVMI factor solutions is discussed by comparing with the more accurate analytical-Ritz solutions presented in this paper. Furthermore, It is seen that the present method is also suitable for the vibration analysis of rectangular plates in contact with infinite fluid by taking the finite, but larger size fluid domain as an approximation in the computation.

1. INTRODUCTION

THE INTERACTION OF FLUID AND PLATE has been a topic of interest among researchers (Lamb 1921; Meyerhoff 1970; Amabili *et al.* 1995) for many years. It is obvious that a plate in contact with fluid behaves differently from the plate in air. The existing investigations to fluid–plate interaction show that the natural frequencies of a plate in contact with fluid decrease significantly compared with those in air, especially for the fundamental frequency. Various methods have been applied to resolve the problem of fluid–plate interaction, such as analytical methods (Bauer 1981; Soedel & Soedel 1994), semi-analytical methods (Cheung *et al.* 1985; Amabili *et al.* 1996) and numerical methods (Hylarides & Vorus 1982; Marcus 1978). There is no doubt that numerical methods such as finite element and boundary element can resolve the problems of fluid–plate interaction; however, the modelling, code preparation and numerical computation require a long time. While the analytical method can give exact or accurate solutions, it is however limited to very special and simple cases. Semi-analytical methods, which combine the advantages of wide applicability of the numerical method and the high accuracy of the analytical method, can solve the problems at a small computational cost.

0889–9746/00/040339 + 19 $35.00/0

A review of the literature reveals that most of the studies on fluid–plate interaction are about circular plates. For example, Kwak (1991) used Hankel transformation to obtain the nondimensional added virtual mass incremental (NAVMI) factors for a circular plate placed on the free fluid surface of an infinite fluid domain. The same problem was considered by Amabili *et al.* (1995) to analyse the effect of Poisson's ratio on NAVMI factors in detail. Some further investigations on circular and annular plates in contact with fluid in an infinite domain were carried out by Amabili (1996), Amabili & Kwak (1996) and Amabili (1996). Chiba (1993, 1994) studied the axisymmetric vibration of the elastic bottom in a cylindrical tank filled with fluid by considering the effects of elastic foundation and hydrostatic pressure. Nagaya & Takeuchi (1984) studied the vibration of the bottom in an arbitrarily shaped cylindrical container filled with fluid. In comparison, the investigation on the vibration of rectangular plates in contact with fluid is very limited. Bauer (1981) studied the vibration of a simply supported elastic bottom in a rectangular tank filled with fluid. Marcus (1978), and Fu & Price (1987) studied the vibration of vertical or horizontal cantilevered rectangular plates immersed in fluid. Soedel & Soedel (1994) studied the free and forced vibration of a simply supported rectangular plate carrying liquid with reservoir conditions at its edges. Recently, Kwak (1996) further studied the NAVMI factors of rectangular plates acted upon by water in an infinite domain by using the Rayleigh–Ritz method combined with the Green function method. No work concerning the problem studied in the present paper has been found in the open literature by the authors.

In this paper, an analytical-Ritz method is developed to analyse the interaction of horizontal rectangular plates in contact with fluid on one side. The elastic rectangular plate is considered as a part of the rigid bottom of a rectangular container, and its edges are parallel to those of the bottom. The high accuracy and small computational cost of the method proposed herein are demonstrated by the convergency studies. The accuracy of the AVMI factor solutions are examined, and the effects of fluid–plate size and density ratios on the natural frequencies of the fluid–plate system are studied in detail. It can be seen that the method proposed is also applicable for analysing the vibration of a rectangular plate in contact with fluid in an infinite domain by taking a finite but larger size fluid domain as a replacement in the computation.

2. PROBLEM OF INVESTIGATION

Let us consider a rectangular plate with width a, length b, thickness t_p, and mass density ρ_p, which is a part of the horizontal rigid bottom of a rectangular container filled with fluid, as shown in Figure 1. The width and length of the bottom are c and d, respectively. The container has four vertical rigid walls. The plate is assumed to be made of homogeneous and isotropic material. The effects of shear deformation and rotary inertia are not considered, so the Kirchhoff theory of plate vibration is applicable. The fluid with depth h and mass density ρ_f is considered to be incompressible, inviscid and irrotational. The fluid–plate system has two families of modes: the sloshing and the bulging ones. The sloshing modes are caused by the oscillation of the fluid free surface due to the rigid body movement of the container (these modes can also be affected by the flexibility of the container but are characteristic of a rigid tank). In this case, the amplitude of the free surface wave is dominant over that of the plate vibration, and when the fluid-dominated modes (sloshing modes) are in resonance, the kinetic and potential vibration energies are mainly in the fluid. On the other hand, the bulging modes are related to the vibration of the flexible plate which moves the fluid. In such a case, the amplitude of the plate vibration is dominant over that of the free surface wave, and when the plate-dominated modes (bulging modes) are in resonance, the potential vibration energy is mainly in the form of strain energy in the plate. Here our

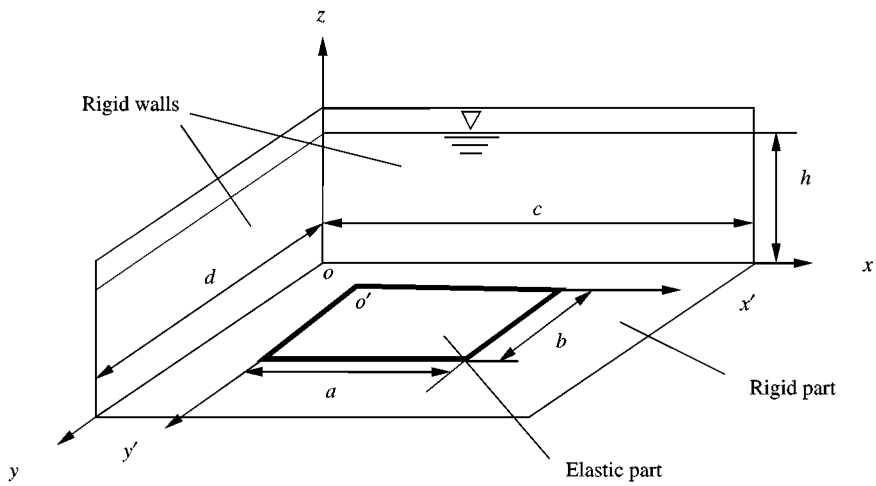

Figure 1. Geometry of the fluid–plate interaction and coordinate system.

attention is focused on the analysis of the bulging modes, which are very important for structural designers because failures of elastic plates in fatigue are most likely to be due to plate-dominated mode resonances. It is also well known that the influence of free surface waves on bulging modes of structures which are not very flexible (Amabili & Dalpiaz 1998; Kondo 1981) is low and for many applications involving primarily bulging modes the simplified free surface condition (zero dynamic pressure) can be applied with sufficient accuracy.

Two sets of Cartesian coordinates ($oxyz$ and $o'x'y'z$), whose corresponding axes are parallel to each other, are developed to describe the motion of the fluid and the vibration of the plate, respectively. The origin o' of the coordinate system $o'x'y'z$ is located at $(x_0, y_0, 0)$ in the coordinate system $oxyz$, which describes the location of the plate on the bottom. The dynamic deformation of the plate in the z direction is expressed by $w(x', y', t)$.

3. MOTION OF THE FLUID

The motion of the fluid can be described by the velocity potential $\phi(x, y, z, t)$ and satisfies the Laplace equation as follows:

$$\frac{\partial^2\phi}{\partial x^2} + \frac{\partial^2\phi}{\partial y^2} + \frac{\partial^2\phi}{\partial z^2} = 0 \quad \text{in } V_f, \tag{1}$$

where V_f represents the fluid domain. The relations between velocity potential and velocity of the fluid are: $v_x = -\partial\phi/\partial x$, $v_y = -\partial\phi/\partial y$, $v_z = -\partial\phi/\partial z$.

The conditions of the four vertical impermeable rigid walls of the container are given by

$$\frac{\partial\phi}{\partial x} = 0 \quad x = 0, c, \quad z = 0 \text{ to } h, \tag{2, 3}$$

The condition of neglecting surface waves implies zero dynamic pressure on the free surface,

$$\frac{\partial\phi}{\partial t} = 0, \qquad z = h. \tag{4}$$

The condition on the horizontal bottom, a part of which is elastic and the rest rigid, is expressed by

$$-\left.\frac{\partial \phi}{\partial z}\right|_{z=0} = \begin{cases} \dfrac{\partial w}{\partial t}, & x_0 \le x \le x_0 + a, \quad y_0 \le y \le y_0 + b, \\ 0, & \text{the other parts of the bottom.} \end{cases} \tag{5}$$

Assuming that the solution of $\phi(x, y, z, t)$ has the form of

$$\phi = X(x)\,Y(y)\,Z(z)\,\dot{T}(t), \tag{6}$$

and applying the method of separation of variables to equation (1), gives the following three uncoupled, second-order, ordinary differential equations

$$\frac{\mathrm{d}^2 X}{\mathrm{d}x^2} \pm p_x^2 X = 0, \tag{7}$$

$$\frac{\mathrm{d}^2 Y}{\mathrm{d}y^2} \pm p_y^2 Y = 0, \tag{8}$$

$$\frac{\mathrm{d}^2 Z}{\mathrm{d}z^2} \mp (p_x^2 + p_y^2) Z = 0, \tag{9}$$

where $\dot{T}(t) = \mathrm{d}T(t)/\mathrm{d}t$ and both p_x^2 and p_y^2 are arbitrary nonnegative numbers.

The general solutions of equations (7)–(9) may easily be given from knowledge of ordinary differential equations. Further, considering the boundary conditions (2)–(4), one obtains the solution of the velocity potential of the fluid as follows:

$$\phi(x, y, z, t) = h\dot{T}(t) \sum_{m=0}^{\infty} \sum_{n=0}^{\infty} A_{mn} \cos(m\pi\xi) \cos(n\pi\eta) F_{mn}(\zeta), \tag{10}$$

where A_{mn} ($m, n = 0, 1, 2, \ldots$) are the unknown constants and

$$F_{mn}(\zeta) = \begin{cases} 1 - \zeta, & m = n = 0, \\ \mathrm{e}^{q_{mn}\zeta} - \mathrm{e}^{q_{mn}(2-\zeta)}, & \text{the other } m \text{ and } n, \end{cases} \tag{11}$$

in which

$$q_{mn} = \pi\beta\sqrt{(m/\alpha)^2 + n^2}\,. \tag{12}$$

In the above equations, the following nondimensional parameters and coordinates are introduced:

$$\alpha = c/d, \quad \beta = h/d, \quad \xi = x/c, \quad \eta = y/d, \quad \zeta = z/h. \tag{13}$$

Assuming that the solution of the dynamic deformation of the plate is in the form of

$$w(x', y', t) = W(x', y')\,T(t), \tag{14}$$

and substituting equations (10) and (14) into equation (5) gives

$$\sum_{m=0}^{\infty} \sum_{n=0}^{\infty} A_{mn} \cos(m\pi\xi) \cos(n\pi\eta) F'_{mn}(\zeta)|_{\zeta=0} = \begin{cases} -W(x', y'), & \xi_0 \le \xi \le \xi_0 + \lambda, \eta_0 \le \eta \le \eta_0 + \gamma, \\ 0, & \text{the other parts of the bottom,} \end{cases} \tag{15}$$

where

$$F'_{mn}(\zeta) = \begin{cases} -1, & m = n = 0, \\ q_{mn}[e^{q_{mn}\zeta} + e^{q_{mn}(2-\zeta)}], & \text{the other } m \text{ and } n, \end{cases} \tag{16}$$

in which the following nondimensional parameters and coordinates are also used:

$$\lambda = a/c, \quad \gamma = b/d, \quad \xi_0 = x_0/c, \quad \eta_0 = y_0/d. \tag{17}$$

Applying the double Fourier series expansion to the two sides of equation (15) in the domain $0 \le \xi \le 1$, $0 \le \eta \le 1$, the coefficients A_{mn} can be derived exactly in the form of integral equations, such that

$$A_{mn} = \frac{\varepsilon_{mn}}{Q_{mn}} I_{mn}, \tag{18}$$

where

$$\varepsilon_{mn} = \begin{cases} 1, & m = 0, n = 0, \\ 2, & m = 0,\ n \neq 0 \text{ or } m \neq 0,\ n = 0, \\ 4, & \text{the other } m \text{ and } n, \end{cases} \tag{19}$$

$$Q_{mn} = \begin{cases} 1, & m = 0,\ n = 0, \\ -q_{mn}(1 + e^{2q_{mn}}), & \text{the other } m \text{ and } n, \end{cases} \tag{20}$$

$$I_{mn} = \int_{\xi_0}^{\xi_1} \int_{\eta_0}^{\eta_1} W(x', y') \cos(m\pi\xi) \cos(n\pi\eta)\, d\xi\, d\eta. \tag{21}$$

In the above equations, $\xi_1 = \xi_0 + \lambda$ and $\eta_1 = \eta_0 + \gamma$. Finally, the velocity potential of the fluid is given by

$$\phi = h\dot{T}(t) \sum_{m=0}^{\infty} \sum_{n=0}^{\infty} \frac{\varepsilon_{mn}}{Q_{mn}} I_{mn} \cos(m\pi\xi) \cos(n\pi\eta) F_{mn}(\zeta). \tag{22}$$

It should be mentioned that the integrals I_{mn} include the unknown dynamic deformation $W(x', y')$ of the plate, which will be dealt with later.

4. ENERGY FUNCTIONAL OF THE SYSTEM

Because of the hypothesis of the incompressible, inviscid, irrotational fluid and no surface waves, only kinetic energy can be attributed to the fluid when the plate vibrates, which is expressed by T_f, as follows:

$$T_f = \frac{1}{2} \rho_f \iiint_{V_f} (\nabla\phi)^2\, dv. \tag{23}$$

Considering equation (1) and applying Green's theorem to the above equation, the volume integration can be transformed into a surface integration surrounding the fluid domain (Lamb 1945), as follows:

$$T_f = \frac{1}{2} \rho_f \oiint_{S_f} \phi \nabla\phi \cdot \mathbf{n}\, ds. \tag{24}$$

where S_f represents the surface of the fluid domain, and **n** is the outward vector normal to the fluid surface. Further considering the boundary conditions (2)–(5), one has

$$T_f = \frac{1}{2}\rho_f\, hdc\dot{T}(t)^2 \sum_{m=0}^{\infty}\sum_{n=0}^{\infty} \frac{\varepsilon_{mn}}{Q_{mn}} I_{mn}^2 \bar{F}_{mn}, \tag{25}$$

in which

$$\bar{F}_{mn} = \begin{cases} 1, & m = 0,\ n = 0, \\ 1 - e^{2q_{mn}}, & \text{the other } m \text{ and } n. \end{cases} \tag{26}$$

It is well known that both kinetic energy and strain energy can be attributed to the plate, which are expressed by T_p and U_p, respectively, as follows:

$$T_p = \frac{1}{2}\rho_p t_p \dot{T}(t)^2 \int_0^a \int_0^b W(x', y')^2 \,dy'\,dx', \tag{27}$$

$$U_p = \frac{1}{2} DT(t)^2 \int_0^a \int_0^b \left\{ \left(\frac{\partial^2 W}{\partial x^2}\right)^2 + 2\frac{\partial^2 W}{\partial x'^2}\frac{\partial^2 W}{\partial y'^2} + \left(\frac{\partial^2 W}{\partial y'^2}\right)^2 \right.$$
$$\left. -2(1-v)\left[\frac{\partial^2 W}{\partial x'^2}\frac{\partial^2 W}{\partial y'2} - \left(\frac{\partial^2 W}{\partial x'\partial y'}\right)^2\right]\right\} dy'\,dx'. \tag{28}$$

where v is the Poisson's ratio and $D = Et_p^3/[12(1-v^2)]$ is the flexural rigidity of the plate.
Hence, the Lagrangian function of the fluid–plate system for free vibration is

$$\Pi = (T_p)_{\max} + (T_f)_{\max} - (U_p)_{\max}. \tag{29}$$

5. FREQUENCY EQUATION

When the plate undergoes free vibration, $T(t)$ is a simple harmonic function. Assume that the dynamic deformation of the plate is in the form of

$$W(x', y') = \sum_{j=1}^{J}\sum_{l=1}^{L} C_{jl} f_j(x') g_l(y'), \tag{30}$$

where C_{jl} are the unknown constants, J and L are the truncated orders of the series and $f_j(x')$, $g_l(y')$ are the admissible functions in the x' and y' directions, respectively.
Substituting equation (30) into equation (29) and applying the Ritz approach, one has

$$\frac{\partial \Pi}{\partial C_{jl}} = 0, \qquad j = 1, 2, \ldots, J, \quad l = 1, 2, \ldots, L, \tag{31}$$

which results in

$$\sum_{j=1}^{J}\sum_{l=1}^{L} [K_{jl\bar{j}\bar{l}} - \Omega^2(M_{jl\bar{j}\bar{l}} + \tilde{M}_{jl\bar{j}\bar{l}})]C_{jl} = 0,$$
$$\bar{j} = 1, 2, \ldots, J, \quad \bar{l} = 1, 2, \ldots, L, \tag{32}$$

where

$$K_{jl\bar{j}\bar{l}} = E_{j\bar{j}}^{(2,2)} F_{l\bar{l}}^{(0,0)} + \mu^4 E_{j\bar{j}}^{(0,0)} F_{l\bar{l}}^{(2,2)} + \nu\mu^2 (E_{j\bar{j}}^{(0,2)} F_{l\bar{l}}^{(2,0)} + E_{j\bar{j}}^{(2,0)} F_{l\bar{l}}^{(0,2)}$$

$$+ 2(1-\nu)\mu^2 E_{j\bar{j}}^{(1,1)} F_{l\bar{l}}^{(1,1)}, \quad \Omega^2 = \rho_p t_p \omega^2 a^4/D, \quad \mu = a/b, \tag{33}$$

$$M_{jl\bar{j}\bar{l}} = E_{j\bar{j}}^{(0,0)} F_{l\bar{l}}^{(0,0)}, \quad \tilde{M}_{jl\bar{j}\bar{l}} = \frac{\tau\beta}{\sigma\lambda\gamma^2} \sum_{m=0}^{\infty} \sum_{n=0}^{\infty} \frac{\varepsilon_{mn}}{Q_{mn}} \bar{F}_{mn} \tilde{E}_{mj} \tilde{E}_{m\bar{j}} \tilde{F}_{nl} \tilde{E}_{n\bar{l}},$$

in which ω is the radian natural frequency of the fluid–plate system, and

$$E_{j\bar{j}}^{(r,s)} = \int_0^1 (\mathrm{d}^r f_j(\xi')/\mathrm{d}\xi'^r)(\mathrm{d}^s f_{\bar{j}}(\xi')/\mathrm{d}\xi'^s)\,\mathrm{d}\xi',$$

$$F_{l\bar{l}}^{(r,s)} = \int_0^1 (\mathrm{d}^r g_l(\eta')/\mathrm{d}\eta'^r)(\mathrm{d}^s g_{\bar{l}}(\eta')/\mathrm{d}\eta'^s)\,\mathrm{d}\eta',$$

$$r, s = 0, 1, 2, \quad \tilde{E}_{mj} = \int_{\xi_0}^{\xi_1} f_j(\xi') \cos(m\pi\xi)\,\mathrm{d}\xi,$$

$$\tilde{F}_{nl} = \int_{\eta_0}^{\eta_1} g_l(\eta') \cos(n\pi\eta)\,\mathrm{d}\eta,$$

$$\tau = \frac{\rho_f}{\rho_p}, \qquad \sigma = t_p/b, \qquad \xi' = x'/a, \qquad \eta' = y'/b, \tag{34}$$

It is obvious that the matrix $\tilde{M}$, made up of elements $\tilde{M}_{jl\bar{j}\bar{l}}$, represents the coupling effect of fluid–plate interaction, which is equivalent to a generalized distributed mass attached to the plate and is called added virtual mass incremental (AVMI) matrix (Kwak 1996). It can be seen that equation (32) is a standard eigenvalue problem; the dimensionless frequency parameters Ω_i ($i = 1, 2, \dots, J \times N$) and the coefficients C_{jl} ($j = 1, 2, \dots, J$, $l = 1, 2, \dots, L$) corresponding to every Ω_i can be easily obtained by using a standard eigenvalue program. Substituting the results into equation (30) gives the corresponding modes. It should be noted that when calculating the integrals $\tilde{E}_{mj}$ and $\tilde{F}_{nl}$ in equations (34), the relations $\xi' = (\xi - \xi_0)/\lambda$ and $\eta' = (\eta - \eta_0)/\gamma$ should be used.

For the rectangular plate considered here, the beam eigenfunctions are adopted as the admissible functions, which can be written in a general form of

$$f_j(\xi') = a_j \sin(k_j\xi') + b_j \cos(k_j\xi') + c_j \sinh(k_j\xi') + d_j \cosh(k_j\xi'), \tag{35}$$

in which, the constants a_j, b_j, c_j, d_j and the eigenvalue k_j may be determined by the boundary conditions (corresponding to those of the plate) of the beam. For example, for a simply supported beam, one has

$$a_j = 1, \quad b_j = c_j = d_j = 0, \qquad k_j = j\pi. \tag{36}$$

and for a clamped beam, one has

$$a_j = (\cosh k_j - \cos k_j)/(\sinh k_j - \sin k_j),$$

$$b_j = -1, \quad c_j = -a_j, \quad d_j = 1, \quad \cos k_j \cosh k_j = 1. \tag{37}$$

Similarly, the $g_l(\eta')$ can also be given, but they are not listed here.

6. NUMERICAL RESULTS

In order to check the accuracy and applicability of the approach proposed in this paper, some numerical examples are given for simply supported and fully clamped square plates ($\mu = 1$). In all the computations, unless otherwise stated, five vibrating beam functions and the following dimensionless parameters are used: Poisson's ratio $v = 0{\cdot}3$, fluid–plate density ratio $\tau = 0{\cdot}125$ and plate thickness ratio $\sigma = 0{\cdot}05$. Moreover, the dimensionless radian natural frequency of the plate in air is represented by $\bar{\Omega}$.

6.1. Convergence Study

Examining equations (32) and (33), one can find that the accuracy of the results are concerned with both the truncated orders J and L of the vibrating beam functions and the number of terms of the series summing about m and n. Tables 1 and 2 present the convergence studies on the dimensionless natural frequency Ω, respectively, for simply supported and fully clamped square plates ($\lambda = \gamma$) in contact with a cubic volume of fluid (meaning that $h = c = d$) with respect to the truncated orders of vibrating beam functions. The plates are placed on the middle of the bottom [$\xi_0 = \eta_0 = (1 - \lambda)/2$]. Considering the symmetry of the fluid–plate system, the same numbers of vibrating beam functions in the x' and y' directions are used, which are increased steadily from 1 to 5 with an increment of 2, to demonstrate the monotonic downward convergence behaviour of Ω.

It is seen that the speed of convergence is very rapid, and in general 3–5 terms of the vibrating beam functions will give the first six natural frequencies of the system with sufficiently high accuracy. One can also find that both the convergence speed and the accuracy are basically unaffected by the fluid–plate size ratio λ (or γ), this means that only a small size matrix needs to be calculated for all cases. Furthermore, the results show that the natural frequencies of the fluid–plate system approach constant values quickly with the decrease of the fluid–plate size ratio λ ($\lambda = \gamma = 0$ means a semi-infinite fluid domain). When $\lambda = \gamma = \frac{1}{256}$, the results have already been very close to values given by Kwak (1996) for the baffled plates in contact with infinite fluid domain. This implies that the errors will be very small and can be controlled if a fluid domain of infinite size (infinite width and/or length and/or depth) is replaced by a fluid domain of finite, but larger size.

Table 3 presents the convergence studies on the eigenvalue Ω for the same objects as the foregoing with respect to the number of terms in the double series summing about m and n. Owing to the symmetry of the system, the same number of terms about m and n are also used. From the table, one can see that the number of terms in the series for obtaining satisfactory results are dependent on the size ratio of the fluid–plate system. The smaller the fluid–plate size ratio, the higher is the number of terms needed in the series. However, stable numerical computation can always be ensured because of the excellent performance of the Fourier series expansion.

6.2. AVMI factor Solution

If the admissible functions of the plate in contact with fluid are selected as the exact modes of the plate in air and if also the AVMI matrix $\tilde{M}$ is a diagonal one ($\tilde{M}_{ij} = 0$, for $i \neq j$), then the wet modes of the plate are the same as those of the plate in air (dry modes). In this case, the analysis can be greatly simplified and the dimensionless natural frequencies of the fluid–plate interaction can easily be obtained by the formula $\tilde{\Omega}_i = \bar{\Omega}_i/\sqrt{1 + \tilde{M}_{ii}/M_{ii}}$, in which, M_{ii} are the ith diagonal elements of mass matrix M of the plate in air and $\tilde{M}_{ii}$, called

TABLE 1

The convergence study of natural frequency for a simply supported square plate in contact with a cubic volume of fluid by using a different number of vibrating beam functions

$J = L$	Ω_1	Ω_2	Ω_3	Ω_4	Ω_5	Ω_6
$\lambda = \gamma = 1$, $m = n = 30$						
1	11·858					
3	11·844	39·255	39·255	66·633	81·702	85·685
5	11·844	39·243	39·243	66·609	81·643	85·674
$\lambda = \gamma = \frac{1}{2}$, $m = n = 40$						
1	12·878					
3	12·870	40·722	40·722	68·393	83·744	86·774
5	12·870	40·718	40·718	68·389	83·716	86·770
$\lambda = \gamma = \frac{1}{4}$, $m = n = 50$						
1	13·365					
3	13·360	40·878	40·878	68·441	84·362	86·800
5	13·360	40·875	40·875	68·437	84·341	86·797
$\lambda = \gamma = \frac{1}{8}$, $m = n = 80$						
1	13·615					
3	13·611	40·898	40·898	68·444	84·652	86·803
5	13·611	40·895	40·895	68·439	84·633	86·800
$\lambda = \gamma = \frac{1}{16}$, $m = n = 150$						
1	13·744					
3	13·740	40·900	40·900	68·443	84·799	86·805
5	13·740	40·897	40·897	68·440	84·781	86·801
$\lambda = \gamma = \frac{1}{128}$, $m = n = 1500$						
1	13·859					
3	13·855	40·900	40·900	68·443	84·927	86·802
5	13·855	40·897	40·897	68·439	84·911	86·798
$\lambda = \gamma = \frac{1}{256}$, $m = n = 2000$						
1	13.867					
3	13.864	40·901	40·901	68·446	84·944	86·810
5	13·863	40·898	40·898	68·442	84·928	86·807
$\lambda = \gamma = 0$						
(Kwak 1996)	13·871	40·903	40·903	68·461		
Plate in air						
Exact	19·739	49·348	49·348	78·957	98·696	98·696

TABLE 2

The convergence study of natural frequency for a fully clamped square plate in contact with a cubic volume of fluid using a different number of vibrating beam functions

$J = L$	Ω_1	Ω_2	Ω_3	Ω_4	Ω_5	Ω_6
$\lambda = \gamma = 1$, $m = n = 30$						
1	23·365					
3	23·121	60·410	60·410	94·240	109·04	116·15
5	23·097	60·293	60·293	93·645	108·65	115·96
$\lambda = \gamma = \frac{1}{2}$, $m = n = 40$						
1	24·885					
3	24·683	61·803	61·803	95·588	111·74	116·98
5	24·662	61·691	61·691	95·009	111·47	116·82
$\lambda = \gamma = \frac{1}{4}$, $m = n = 50$						
1	25·624					
3	25·438	61·955	61·955	95·622	112·73	117·00
5	25·419	61·848	61·848	95·046	112·48	116·84
$\lambda = \gamma = \frac{1}{8}$, $m = n = 80$						
1	26·002					
3	25·824	61·974	91·974	95·624	113·20	117·00
5	25·805	61·867	61·867	95·047	112·97	116·84
$\lambda = \gamma = \frac{1}{16}$, $m = n = 150$						
1	26·195					
3	26·022	61·976	61·976	95·624	113·44	117·00
5	26·003	61·869	61·869	95·047	113·22	116·84
$\lambda = \gamma = \frac{1}{128}$, $m = n = 1500$						
1	26·367					
3	26·197	61·977	61·977	95·624	113·66	117·00
5	26·179	61·869	61·869	95·047	113·44	116·84
$\lambda = \gamma = \frac{1}{256}$, $m = n = 2000$						
1	26·379					
3	26·210	61·977	61·977	95·625	113·68	117·00
5	26·192	61·870	61·870	95·049	113·46	116·84
$\lambda = \gamma = 0$						
(Kwak 1996)	26·319	62·051	62·051	95·230		
Plate in air						
5	35·991	73·420	73·420	108·37	131·64	132·24

TABLE 3

The convergence study of natural frequency for the simply supported and fully clamped square plates in contact with a cubic volume of fluid using different numbers of summing terms in series; five vibrating beam functions are used in each direction

$m = n$	Ω_1	Ω_2	Ω_3	Ω_4	Ω_5	Ω_6
SSSS $\lambda = \gamma = 1$						
20	11·844	39·243	39·243	66·609	81·644	85·674
50	11·844	39·243	39·243	66·609	81·643	85·674
$\lambda = \gamma = \frac{1}{2}$						
20	12·870	40·718	40·718	68·390	83·718	86·773
50	12·870	40·718	40·718	68·389	83·716	86·770
$\lambda = \gamma = \frac{1}{4}$						
20	13·360	40·887	40·887	68·471	84·398	86·862
50	13·359	40·875	40·875	68·437	84·341	86·797
120	13·359	40·875	40·875	68·436	84·340	86·796
$\lambda = \gamma = \frac{1}{8}$						
20	13·625	41·500	41·500	70·228	90·663	93·352
50	13·611	40·899	40·899	68·451	84·653	86·823
120	13·610	40·894	40·894	68·438	84·631	86·797
$\lambda = \gamma = \frac{1}{16}$						
20	14·367	46·003	46·003	77·530	95·185	98·294
50	13·746	41·007	41·007	68·764	87·258	89·573
120	13·740	40·898	40·898	68·443	84·789	86·809
CCCC, $\lambda = \gamma = 1$						
20	23·097	60·263	60·263	93·645	108·65	115·96
50	23·097	60·263	60·263	93·645	108·65	115·96
$\lambda = \gamma = \frac{1}{2}$						
20	24·662	61·692	61·692	95·009	111·47	116·82
50	24·662	61·691	61·691	95·009	111·47	116·82
$\lambda = \gamma = \frac{1}{4}$						
20	25·420	61·860	61·860	95·091	112·59	116·96
50	25·419	61·848	61·848	95·046	112·48	116·84
120	25·419	61·848	61·848	95·046	112·48	116·84
$\lambda = \gamma = \frac{1}{8}$						
20	25·890	63·413	63·413	98·814	121·73	126·49
50	25·806	61·868	61·868	95·052	113·00	116·87
120	25·805	61·866	61·866	95·047	112·97	116·84
$\lambda = \gamma = \frac{1}{16}$						
20	27·579	69·855	69·855	107·18	125·36	131·30
50	26·010	62·262	62·262	96·092	117·78	121·92
120	26·003	61·870	61·870	95·050	113·22	116·85

AVMI factors (Lamb 1921; Kwak 1991), are those of AVMI matrix $\tilde{M}$ of the fluid. The AVMI matrices for a simply supported square plate placed on the middle of the bottom and in contact with a cubic volume of fluid are given by using two vibrating beam functions in each direction, as follows:

$$\tilde{M}=\begin{bmatrix} 4{\cdot}428\times10^{-1} & -2{\cdot}263\times10^{-17} & -2{\cdot}266\times10^{-17} & 1{\cdot}176\times10^{-33} \\ -2{\cdot}263\times10^{-17} & 1{\cdot}449\times10^{-1} & 1{\cdot}176\times10^{-33} & -8{\cdot}247\times10^{-18} \\ -2{\cdot}263\times10^{-17} & 1{\cdot}176\times10^{-33} & 1{\cdot}449\times10^{-1} & -8{\cdot}216\times10^{-18} \\ 1{\cdot}176\times10^{-33} & -8{\cdot}247\times10^{-18} & -8{\cdot}216\times10^{-18} & 1{\cdot}010\times10^{-1} \end{bmatrix} \quad (38)$$

for $\lambda=\gamma=1$,

$$\tilde{M}=\begin{bmatrix} 3{\cdot}374\times10^{-1} & -9{\cdot}325\times10^{-18} & -9{\cdot}452\times10^{-18} & 3{\cdot}367\times10^{-34} \\ -9{\cdot}325\times10^{-18} & 1{\cdot}171\times10^{-1} & 3{\cdot}367\times10^{-34} & -1{\cdot}553\times10^{-18} \\ -9{\cdot}452\times10^{-18} & 3{\cdot}367\times10^{-34} & 1{\cdot}171\times10^{-1} & -1{\cdot}433\times10^{-18} \\ 3{\cdot}367\times10^{-34} & -1{\cdot}533\times10^{-18} & -1{\cdot}433\times10^{-18} & 8{\cdot}319\times10^{-2} \end{bmatrix} \quad (39)$$

for $\lambda=\gamma=\frac{1}{2}$,

$$\tilde{M}=\begin{bmatrix} 2{\cdot}953\times10^{-1} & 1{\cdot}085\times10^{-17} & 1{\cdot}136\times10^{-17} & 1{\cdot}079\times10^{-33} \\ 1{\cdot}085\times10^{-17} & 1{\cdot}143\times10^{-1} & 1{\cdot}079\times10^{-33} & 8{\cdot}181\times10^{-18} \\ 1{\cdot}136\times10^{-17} & 1{\cdot}079\times10^{-33} & 1{\cdot}143\times10^{-1} & 7{\cdot}708\times10^{-18} \\ 1{\cdot}079\times10^{-33} & 8{\cdot}181\times10^{-18} & 7{\cdot}708\times10^{-18} & 8{\cdot}272\times10^{-2} \end{bmatrix} \quad (40)$$

for $\lambda=\gamma=\frac{1}{4}$, and

$$\tilde{M}=\begin{bmatrix} 2{\cdot}755\times10^{-1} & 1{\cdot}827\times10^{-17} & 1{\cdot}818\times10^{-18} & 2{\cdot}957\times10^{-34} \\ 1{\cdot}827\times10^{-17} & 1{\cdot}140\times10^{-1} & 2{\cdot}957\times10^{-34} & -6{\cdot}887\times10^{-19} \\ 1{\cdot}818\times10^{-18} & 2{\cdot}957\times10^{-34} & 1{\cdot}140\times10^{-1} & 1{\cdot}162\times10^{-17} \\ 2{\cdot}957\times10^{-34} & -6{\cdot}887\times10^{-19} & 1{\cdot}162\times10^{-17} & 8{\cdot}270\times10^{-2} \end{bmatrix} \quad (41)$$

for $\lambda=\gamma=\frac{1}{8}$.

From the above four matrices, one can see that they are all nearly diagonal; in fact, the absolute off-diagonal elements are at least 14 orders of magnitude smaller than the diagonal ones, which means that ignoring the off-diagonal elements will not result in large errors. It is clear that more diagonal dominant elements in the matrix $\tilde{M}$ will result in closer solutions to the AVMI factor solutions. When all the off-diagonal elements are approximated as zeros, the AVMI factor solutions can be expressed as $\tilde{\Omega}_i=\bar{\Omega}_i/\sqrt{1+4\tilde{M}_{ii}}$. The percentage errors $e_i=(1-\tilde{\Omega}_i/\Omega_i)\times100$ ($i=1, 2, 3, 4$) of the first four natural frequencies between the AVMI factor solutions and the analytical-Ritz solutions are given in Figure 2. One can see that the maximum absolute error which occurs in $\lambda=\gamma=1$ (in such a case, the bottom is completely elastic) is less than 0·116%. The same conclusion can be reached for the fully clamped square plates. The AVMI matrices for a fully clamped square plate placed on the middle of the bottom and in contact with a cubic volume of fluid are given by using two

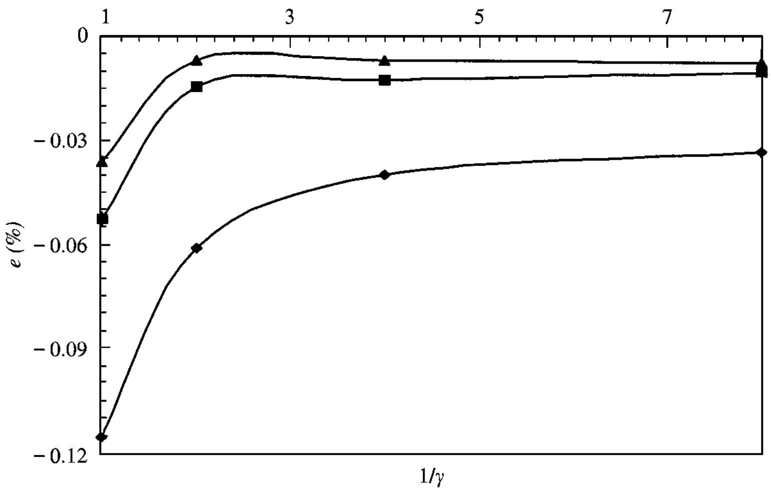

Figure 2. The percentage errors e_i ($i = 1, 2, 3, 4$) of the first four natural frequencies of the AVMI solutions with respect to the analytical-Ritz solutions for a simply supported square plate in contact with a cubic volume of fluid as a function of fluid–plate width ratio γ: —◆—, e_1; —■—, e_2, e_3; —▲—, e_4.

vibrating beam functions in each direction, as follows:

$$\tilde{M} = \begin{bmatrix} 1{\cdot}388 & -4{\cdot}439\times10^{-8} & -4{\cdot}439\times10^{-8} & 2{\cdot}933\times10^{-15} \\ -4{\cdot}439\times10^{-8} & 4{\cdot}734\times10^{-1} & 2{\cdot}933\times10^{-15} & -3{\cdot}115\times10^{-8} \\ -4{\cdot}439\times10^{-8} & 2{\cdot}933\times10^{-15} & 4{\cdot}734\times10^{-1} & -3{\cdot}115\times10^{-8} \\ 2{\cdot}933\times10^{-15} & -3{\cdot}115\times10^{-8} & -3{\cdot}115\times10^{-8} & 3{\cdot}313\times10^{-1} \end{bmatrix} \quad (42)$$

for $\lambda = \gamma = 1$.

$$\tilde{M} = \begin{bmatrix} 1{\cdot}105 & -3{\cdot}995\times10^{-8} & -3{\cdot}995\times10^{-8} & 2{\cdot}703\times10^{-15} \\ -3{\cdot}995\times10^{-8} & 4{\cdot}105\times10^{-1} & 2{\cdot}703\times10^{-15} & -2{\cdot}828\times10^{-8} \\ -3{\cdot}995\times10^{-8} & 2{\cdot}703\times10^{-15} & 4{\cdot}105\times10^{-1} & -2{\cdot}828\times10^{-8} \\ 2{\cdot}703\times10^{-15} & -2{\cdot}828\times10^{-8} & -2{\cdot}828\times10^{-8} & 2{\cdot}967\times10^{-1} \end{bmatrix} \quad (43)$$

for $\lambda = \gamma = \frac{1}{2}$.

$$\tilde{M} = \begin{bmatrix} 9{\cdot}858\times10^{-1} & -3{\cdot}949\times10^{-8} & -3{\cdot}949\times10^{-8} & 2{\cdot}697\times10^{-8} \\ -3{\cdot}949\times10^{-8} & 4{\cdot}038\times10^{-1} & 2{\cdot}697\times10^{-8} & -2{\cdot}820\times10^{-8} \\ -3{\cdot}949\times10^{-8} & 2{\cdot}697\times10^{-8} & 4{\cdot}038\times10^{-1} & -2{\cdot}820\times10^{-8} \\ 2{\cdot}697\times10^{-8} & -2{\cdot}820\times10^{-8} & -2{\cdot}820\times10^{-8} & 2{\cdot}958\times10^{-1} \end{bmatrix} \quad (44)$$

for $\lambda = \gamma = \frac{1}{4}$, and

$$\tilde{M} = \begin{bmatrix} 9{\cdot}285\times10^{-1} & -3{\cdot}944\times10^{-8} & -3{\cdot}944\times10^{-8} & 2{\cdot}697\times10^{-15} \\ -3{\cdot}944\times10^{-8} & 4{\cdot}030\times10^{-1} & 2{\cdot}697\times10^{-15} & -2{\cdot}820\times10^{-8} \\ -3{\cdot}944\times10^{-8} & 2{\cdot}697\times10^{-15} & 4{\cdot}030\times10^{-1} & -2{\cdot}820\times10^{-8} \\ 2{\cdot}697\times10^{-15} & -2{\cdot}820\times10^{-8} & -2{\cdot}820\times10^{-8} & 2{\cdot}958\times10^{-1} \end{bmatrix} \quad (45)$$

for $\lambda = \gamma = \frac{1}{8}$.

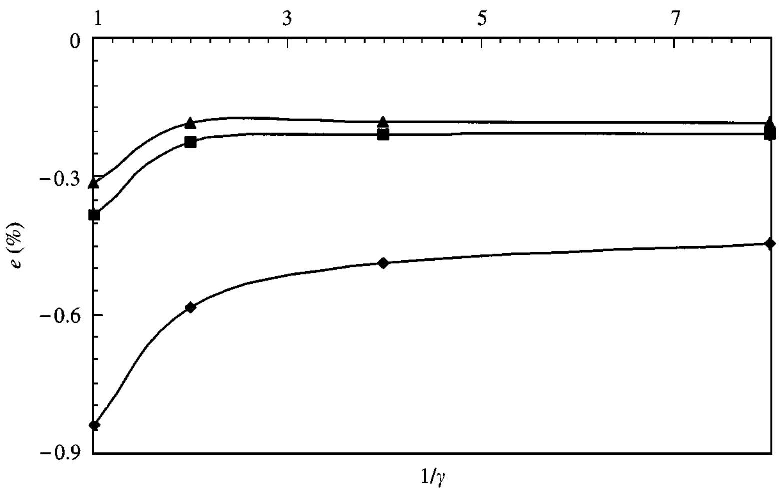

Figure 3. The percentage errors e_i ($i = 1, 2, 3, 4$) of the first four natural frequencies of the AVMI solutions with respect to the analytical-Ritz solutions for a fully clamped square plate in contact with a cubic volume of fluid as a function of fluid–plate width ratio γ: —◆—, e_1; —■—e_2, e_3; —▲—, e_4.

TABLE 4

The first six dimensionless natural frequencies of a square plate in contact wtih a cubic volume of fluid for different locations on the bottom

ξ_0	η_0	Ω_1	Ω_2	Ω_3	Ω_4	Ω_5	Ω_6
SSSS							
0·0	0·0	12·065	39·978	40·146	67·579	82·673	86·214
	$\frac{1}{8}$	12·568	40·357	40·508	68·032	83·320	86·495
	$\frac{1}{4}$	12·739	40·392	40·559	68·043	83·496	86·506
	$\frac{3}{8}$	12·785	40·394	40·569	68·044	83·543	86·508
$\frac{1}{8}$	$\frac{1}{8}$	13·006	40·790	40·814	68·415	83·940	86·782
	$\frac{1}{4}$	13·159	40·828	40·841	68·425	84·108	86·788
	$\frac{3}{8}$	13·197	40·833	40·846	68·427	84·154	86·789
$\frac{1}{4}$	$\frac{1}{4}$	13·288	40·863	40·867	68·434	84·260	86·795
	$\frac{3}{8}$	13·325	40·870	40·871	68·436	84·301	86·759
$\frac{3}{8}$	$\frac{3}{8}$	13·359	40·875	40·875	68·436	84·340	86·796
CCCC							
0·0	0·0	23·381	60·963	61·145	94·389	109·86	116·38
	$\frac{1}{8}$	24·184	61·352	61·497	94·737	110·87	116·60
	$\frac{1}{4}$	24·457	61·370	61·548	94·745	111·18	116·61
	$\frac{3}{8}$	24·530	61·372	61·558	94·746	111·27	116·61
$\frac{1}{8}$	$\frac{1}{8}$	24·868	61·762	61·787	95·029	111·18	116·83
	$\frac{1}{4}$	25·102	61·799	61·814	95·037	112·09	116·83
	$\frac{3}{8}$	25·167	61·805	61·819	95·038	112·17	116·83
$\frac{1}{4}$	$\frac{1}{4}$	25·308	61·835	61·840	95·044	112·35	116·84
	$\frac{3}{8}$	25·365	61·842	61·843	95·045	112·42	116·84
$\frac{3}{8}$	$\frac{3}{8}$	25·419	61·848	61·848	95·046	112·48	116·84

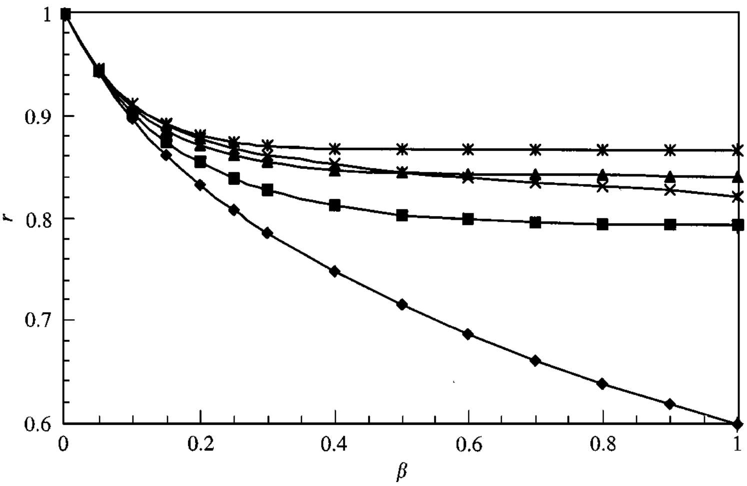

Figure 4. The ratios r_i ($i = 1, 2, \ldots, 6$) of the first six natural frequencies of a simply supported square plate in contact with fluid with respect to those in air as a function of depth ratio β of the fluid: —◆—, r_1; —■—, r_2, r_3; —▲—, r_4; —×—, r_5; —*—, r_6.

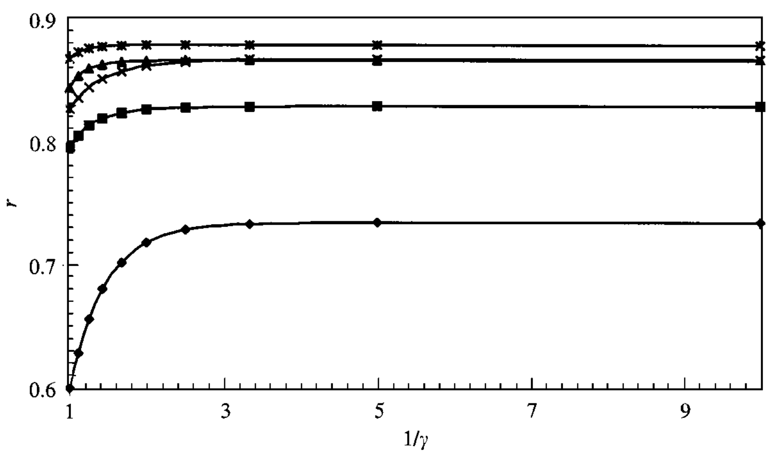

Figure 5. The ratios $r_i (i = 1, 2, \ldots, 6)$ of the first six natural frequencies of a simply supported square plate in contact with fluid with respect to those in air as a function of fluid–plate width (or length) ratio γ ($\lambda = \gamma$) with fluid depth ratio $\beta = \gamma$: —◆—, r_1; —■—, r_2, r_3; —▲—, r_4; —×—, r_5; —*—, r_6.

It can be seen that the off-diagonal elements in the above four matrices are also very small compared to the diagonal ones. Although the dominance of the diagonal for the fully clamped square plate is relatively lower than that of the simply supported square one, the concept of AVMI factor solutions is still applicable in this case. The percentage errors e_i ($i = 1, 2, 3, 4$) of the first four natural frequencies between the AVMI factor solutions and the analytical-Ritz solutions for the fully clamped square plate in contact with fluid by using five vibrating beam functions are given in Figure 3. One can see that the maximum absolute error which occurs in $\lambda = \gamma = 1$ is less than 0·85%. Moreover, it should be mentioned that, because the exact mode solutions for the fully clamped square plate in air cannot be obtained, approximate solutions, which result in a nondiagonal stiffness matrix K, have to

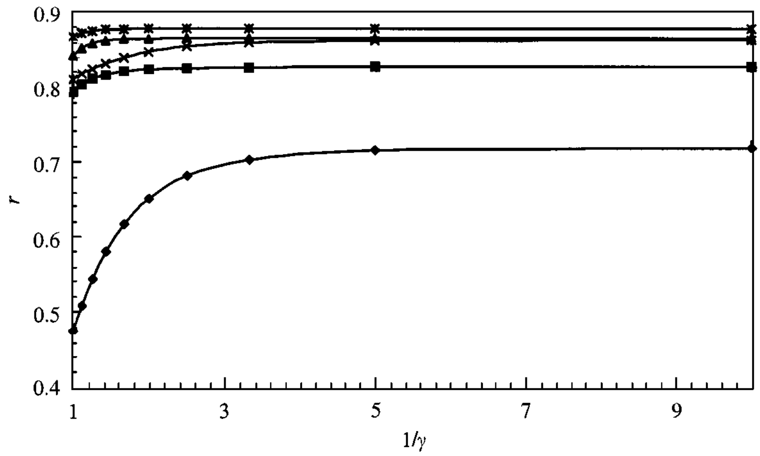

Figure 6. The ratios $r_i (i = 1, 2, \dots, 6)$ of the first six natural frequencies of a simply supported square plate in contact with fluid with respect to those in air as a function of fluid–plate width (or length) ratio γ ($\lambda = \gamma$) with fluid depth ratio $\beta = 2\gamma$: —◆—, r_1; —■—, r_2, r_3; —▲—, r_4; —×—, r_5; —*—, r_6.

be used. In this case, even if the off-diagonal elements in $\tilde{M}$ are neglected, an eigenvalue solution procedure still has to be carried out to obtain the AVMI factor solution $\tilde{\Omega}$.

6.3. Results

As an application example, some numerical results are given in this subsection. The effect of the location of simply supported and fully clamped square plates, placed in the rigid bottom of a square container filled with a cubic volume of fluid, on the first six natural frequencies of the system is studied in Table 4. The side-lengths of the plate are a quarter of the bottom. A careful scrutiny of the results reveals that the closer the plate is to the corner of the bottom, the lower are the natural frequencies; the closer the plate is to the centre of the bottom, the higher are the natural frequencies.

The effect of the depth ratio of the fluid on the first six natural frequencies of the fluid–plate interaction is studied for the simply supported square plates, in which the bottom of the container is entirely occupied by the elastic plate. The ratios $r_i = \Omega_i/\bar{\Omega}_i$ $(i = 1, 2, \dots, 6)$ between the natural frequencies of the "wet" plate and those of the "dry" plate are given in Figure 4, where Ω_1, Ω_5 and Ω_6 are the first three frequencies of double-symmetric modes, Ω_2 and Ω_3 are the frequencies of symmetric–antisymmetric and antisymmetric–symmetric modes, and Ω_4 is the frequency of double-antisymmetric modes. It is seen that the effect of the fluid depth on the first two frequencies of double-symmetric modes Ω_1 and Ω_5, especially on the fundamental frequency Ω_1 is larger than that on the other frequencies. With the increase of the fluid depth, Ω_1 and Ω_5, especially the fundamental frequency Ω_1, monotonically decrease; however, the other frequencies steadily approach constant values. The effect of the horizontal sizes (width and length) of the fluid domain on the first six natural frequencies of the fluid–plate system is studied in Figures 5 and 6 for the simply supported square plates placed on the centre of a square bottom ($\lambda = \gamma$). Two different fluid depths are considered, respectively: $\beta = \gamma$ and $\beta = 2\gamma$. It is seen that with the increase of the horizontal width of the fluid, the natural frequencies of the system decrease steadily to constant values, which once again means that the errors will be very small if a fluid domain of infinite width and length is approximated by a fluid domain of finite but larger width and length.

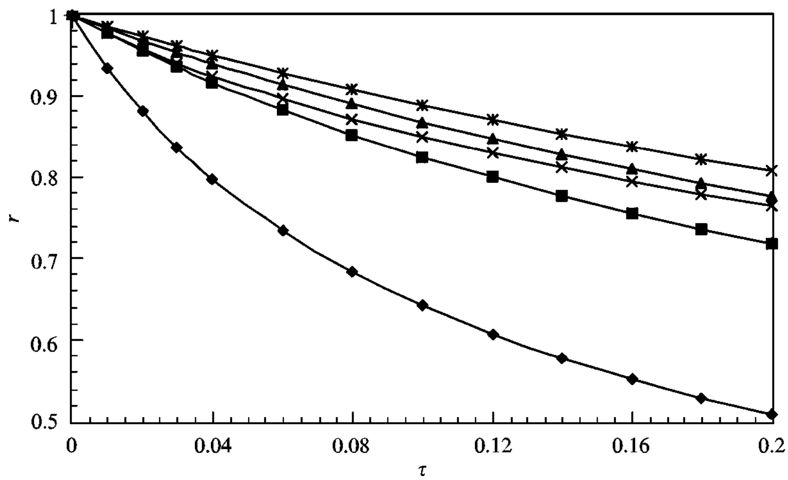

Figure 7. The ratios $r_i (i = 1, 2, \ldots, 6)$ of the first six natural frequencies of a simply supported square plate in contact with a cubic volume of fluid with respect to those in air as a function of fluid–plate density ratio τ: —◆—, r_1; —■—, r_2, r_3; —▲—, r_4; —×—, r_5; —*—, r_6.

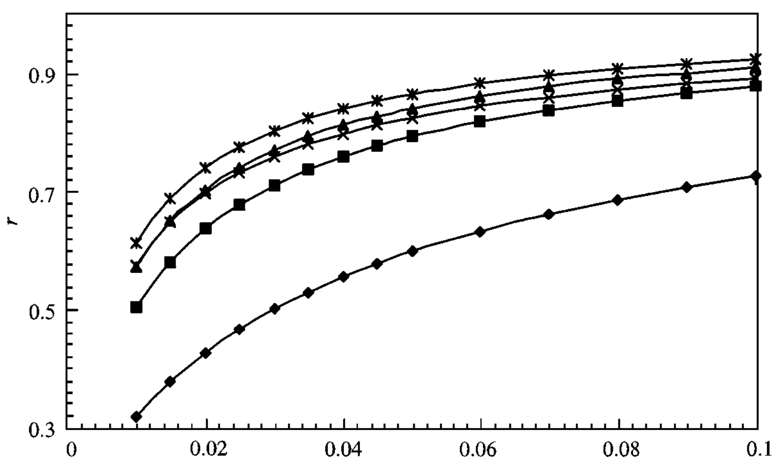

Figure 8. The ratios $r_i (i = 1, 2, \ldots, 6)$ of the first six natural frequencies of a simply supported square plate in contact with a cubic volume of fluid with respect to those in air as a function of thickness ratio σ of the plate: —◆—, r_1; —■—, r_2, r_3; —▲—, r_4; —×—, r_5; —*—, r_6.

In Figure 7, the effect of the fluid–plate density ratio on the first six natural frequencies of the fluid–plate interaction is studied for the simply supported square plates occupying the entire bottom of the container and in contact with a cubic volume of fluid. It is seen that, with the decrease of the fluid–plate density ratio, the natural frequencies of the system monotonically decrease.

The effect of the thickness ratio σ of plates on the first six natural frequencies of the fluid–plate interaction is given in Figure 8 for the simply supported square plates entirely occupying the bottom and in contact with a cubic volume of fluid. It is shown that with the decrease of the thickness ratio of the plate, the natural frequencies of the system will increase monotonically.

7. CONCLUSIONS

The vibratory characteristics of an elastic rectangular plate in contact with fluid on one side are studied in detail. The plate is considered as a part of the rigid bottom of a rectangular container filled with fluid having a free surface. The analytical-Ritz method with highaccuracy and small computational cost is developed to analyse the vibration of the fluid–plate system. The convergence studies demonstrate the high accuracy and the rapid convergence of the approach presented in this paper. In this study, the AVMI factor solutions are also compared with the analytical-Ritz solutions, and the applicability of the AVMI factor solutions is confirmed. The effects of the fluid–plate size and density ratios on the natural frequencies of the system are studied in detail and some interesting conclusions are obtained. The results show that the method is also applicable to a horizontal rectangular plate in contact with an infinite fluid by replacing the infinite fluid with a fluid of finite but larger size in the computations.

ACKNOWLEDGMENTS

The authors wish to thank Professor M. K. Kwak of the Department of Mechanical Design, Kyungnam University, Seoul, Korea, for providing the accurate data used in the figures of his paper (Kwak 1996) for the comparison. This research was supported by the CRCG foundation of the University of Hong Kong.

REFERENCES

AMABILI, M. 1996. Effect of finite fluid depth on the hydroelastic vibrations of circular and annular plates. *Journal of Sound and Vibration* **193,** 909–925.

AMABILI, M. & DALPIAZ, G. 1998. Vibrations of base plates in annular cylindrical tanks: theory and experiments. *Journal of Sound and Vibration* **210,** 329–350.

AMABILI, M., FROSALI, G. & KWAK, M. K. 1996. Free vibrations of annular plates coupled with fluid. *Journal of Sound and Vibration* **191,** 825–846.

AMABILI, M. & KWAK, M. K. 1996. Free vibrations of circular plates coupled with liquids: revising the Lamb problem. *Journal of Fluids and Structures* **10,** 743–761.

AMABILI, M., PASQUALINI, A. & DALPIAZ, G. 1995. Natural frequencies and modes of free-edge circular plates vibrating in vacuum or in contact with liquid. *Journal of Sound and Vibration* **188,** 685–699.

BAUER, H. F. 1981. Hydroelastic vibrations in a rectangular container. *International Journal of Solids and Structures* **17,** 639–652.

CHEUNG, Y. K., CAO, Z. & WU, S. Y. 1985. Dynamic analysis of prismatic structures surrounded by an infinite fluid medium. *Earthquake Engineering and Structural Dynamics* **13,** 351–360.

CHIBA, M. 1993. Nonlinear hydroelastic vibration of a cylindrical tank with an elastic bottom, containing liquid. Part II. linear axisymmetric vibration analysis. *Journal of Fluids and Structures* **7,** 57–73.

CHIBA, M. 1994. Axisymmetric free hydroelastic vibration of a flexural bottom plate in a cylindrical tank supported on an elastic foundation. *Journal of Sound and Vibration* **169,** 387–394.

FU, Y. & PRICE, W. G. 1987. Interactions between a partially or totally immersed vibrating cantilever plate and the surrounding fluid. *Journal of Sound and Vibration* **118,** 495–513.

HYLARIDES, S. & VORUS, W. S. 1982. The added mass matrix in ship vibration, using a source distribution related to the finite element grid of the ship structure. *International Shipbuilding Progress* **29,** 34–43.

KONDO, H. 1981. Axisymmetric vibration analysis of a circular cylindrical tank. *Bulletin of the Japan Society of Mechanical Engineers* **24,** 215–221.

KWAK, M. K. 1991. Vibration of circular plates in contact with water. *Journal of Applied Mechanics* **58,** 480–483.

KWAK, M. K. 1996. Hydroelastic vibration of rectangular plates. *Journal of Applied Mechanics* **63,** 110–115.

LAMB, H. 1921. On the vibrations of an elastic plate in contact with water. *Proceedings of the Royal Society of London* **A 98,** 205–216.

LAMB, H. 1945. *Hydrodynamics*, see p. 46. New York: Dover.

MARCUS, M. S. 1978. A finite-element method applied to the vibration of submerged plates. *Journal of Ship Research* **22,** 94–99.

MEYERHOFF, W. K. 1970. Added masses of thin rectangular plates calculated from potential theory. *Journal of Ship Research* **14,** 100–111.

NAGAYA, K. & TAKEUCHI, J. 1984. Vibration of a plate with arbitrary shape in contact with a fluid. *Journal of the Acoustical Society of America* **75,** 1511–1518.

SOEDEL, S. M. & SOEDEL, W. 1994. On the free and forced vibration of a plate supporting a freely sloshing surface liquid. *Journal of Sound and Vibration* **171,** 159–171.